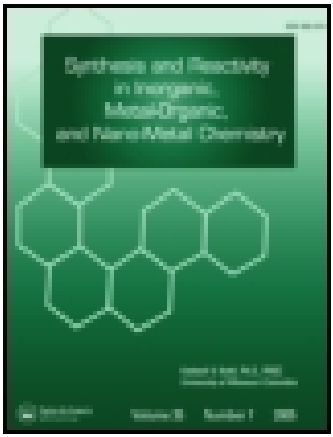

Synthesis and Reactivity in Inorganic and Metal-Organic Chemistry

Publication details, including instructions for authors and subscription information:
http://www.tandfonline.com/loi/lsrt19

Chemistry of Azopyrimidines. Part III. Synthesis, Spectral Characterization and Electrochemical Studies of Arylazopyrimidine Complexes of Palladium(II) and Catecholato Derivatives

R. Roy [a], P. K. Santra [a], D. Das [a], C. Sinha [a], K. Sakata [a] & H. Kuma [a]

[a] Department of Chemistry, The University of Burdwan, Burdwan, 713104, India E-mail:

Published online: 23 Apr 2008.

To cite this article: R. Roy, P. K. Santra, D. Das, C. Sinha, K. Sakata & H. Kuma (2000) Chemistry of Azopyrimidines. Part III. Synthesis, Spectral Characterization and Electrochemical Studies of Arylazopyrimidine Complexes of Palladium(II) and Catecholato Derivatives, Synthesis and Reactivity in Inorganic and Metal-Organic Chemistry, 30:10, 1975-1993, DOI: 10.1080/00945710009351883

To link to this article: http://dx.doi.org/10.1080/00945710009351883

SYNTH. REACT. INORG. MET.-ORG. CHEM., 30(10), 1975–1993 (2000)

CHEMISTRY OF AZOPYRIMIDINES. PART III. SYNTHESIS, SPECTRAL CHARACTERIZATION AND ELECTROCHEMICAL STUDIES OF ARYLAZOPYRIMIDINE COMPLEXES OF PALLADIUM(II) AND CATECHOLATO DERIVATIVES

R. Roy, P. K. Santra, D. Das and C. Sinha*

Department of Chemistry, The University of Burdwan, Burdwan 713104, India
E-mail: bdnuvlib@giascl01.vsnl.net.in

ABSTRACT

2-(Phenylazo)pyrimidine (papm), 2-(*p*-tolylazo)pyrimidine (*p*-tapm), 2-(*p*-chlorophenylazo)pyrimidine (*p*-Clpapm) are used as N,N'-chelators. They are called arylazopyrimidines and abbreviated in general as aapm (**1**). They were reacted with *cis*-$Pd(MeCN)_2Cl_2$ to yield orange-red complexes of the type $Pd(aapm)Cl_2$ (**2**). Upon reaction with catechols in the presence of triethylamine (Et_3N), $Pd(aapm)Cl_2$ yielded the mixed-ligand complexes [Pd(aapm)(O,O)] where O,O = pyrocatecholate [cat, (**3**)], 4-*tert*-butylcatecholate [tbcat, (**4**)], 3,5-di-*tert*-butylcatecholate [dtbcat, (**5**)] and tetrachlorocatecholate [tccat, (**6**)]. The complexes were characterised by elemental analyses, IR spectra, UV-VIS spectra

and ^1H NMR spectra. The redox properties were examined with cyclic voltammetry. [Pd(aapm)(O,O)] exhibits four successive redox responses and the $E_{1/2}$ values are highly sensitive to the nature of the substituents. The electronic spectra of [Pd(aapm)(O,O)] exhibit ligand-to-ligand charge transfer transitions and are different from those of $Pd(aapm)Cl_2$. The band position is largely dependent on the substituent type of the catechol frame and is tentatively assigned to the $3b_1$ (cat) $\rightarrow \pi^*$(aapm) transition.

INTRODUCTION

For the last few years we have been engaged[1-7] in designing ligands with a π-acidic azoimine function, -N=N-C=N-, and in exploration of their coordination chemistry[1-6] and analytical application[7]. Azoimines are isoelectronic with α-diimines and the π-acidity of the ligand depends on the number of heteroatoms, the ring size and the substituents in the heterocyclic ring which regulate the physical and chemical properties of the compounds[8]. The azoimine function is associated with a charge transfer transition from a σ/π-donor unit in a suitable chemical platform[5,6]. Metal complexes of the azoimine function at a lower valent state exhibit metal-to-ligand charge transfer (MLCT) transitions in the azoimine complexes[3,4]. The mixed ligand complexes, [M(azoimine)(O,O)]/[M(diimine)(O,O)] {(M = Pd(II), Pt(II), UO_2(VI); (O,O) = catecholates}, exhibit interesting ligand-to-ligand charge transfer transitions (LLCT)[5,6,9]. The charge transfer takes place from the catecholato center to the azoimine/diimine center. The catecholato transition metal complexes are very interesting[10-16] because of their diverse activities such as redox, magnetic, intercalation, one-dimensional conducting, biological and antitumor properties. This has received continuous interest by the researchers to discover new complexes and examine different properties. The LLCT transition has been studied only recently[5,6,9,15-17]. We have reported earlier the chemistry and spectral properties of Pd(arylazopyridine)(catecholates)[6] and

Pd(arylazoimidazole) (catecholates)[5]. The LLCT transition energy is linearly correlated with the π-acidity of the acceptor ligand and follows the order arylazopyridine > arylazoimidazole. This is due to better π-acidity of pyridine than that of imidazole[8]. To examine the trend of the charge transfer transition energy we have designed arylazopyrimidine [aapm, (**1**)], as a third member in the azoimine family[1,2]. The motif behind the choice of an azopyrimidine derivative is due to the higher π-acidity of pyrimidine than that of pyridine and to the biological/medicinal importance of pyrimidine. In this article we wish to report the synthesis, spectral characterization and electrochemical properties of several palladium(II) complexes of arylazopyrimidines and their dioxolene derivatives.

RESULTS AND DISCUSSION

The arylazopyrimidines and the palladium(II) complexes (**2**)-(**6**) described in this article are shown in Fig. 1. The arylazopyrimidines [aapm, (**1**)] were prepared by condensation of nitrosoaromatics with 2-aminopyrimidine in the presence of Na in dry benzene under refluxing condition[1-2]. They were reacted with *cis*-$Pd(MeCN)_2Cl_2$ in CH_3CN affording orange-red crystalline $Pd(aapm)Cl_2$ (**2**) in high yields. To a $CHCl_3$ solution of $Pd(aapm)Cl_2$ (**2**) added dropwise[5,6] a methanolic solution of catechols in the presence of two equivalents of Et_3N under N_2 atmosphere and stirred for 1 h. The orange-red colour changed to deep brown-violet and the removal of solvents followed by chromatographic purification afforded the catecholate complexes (**3**)-(**6**) in high yields (70-85 %). The composition of the complexes is supported by elemental analyses (Table I).

Spectral Characterization

IR Spectra. IR spectra of [Pd(aapm)(O,O)] (**3**)-(**6**) display single stretching modes at *ca.* 1330 cm^{-1} which are assigned to ν(N=N). In the parent $Pd(aapm)Cl_2$ (**2**) this stretching mode appears at 1380 cm^{-1}. The lowering of the

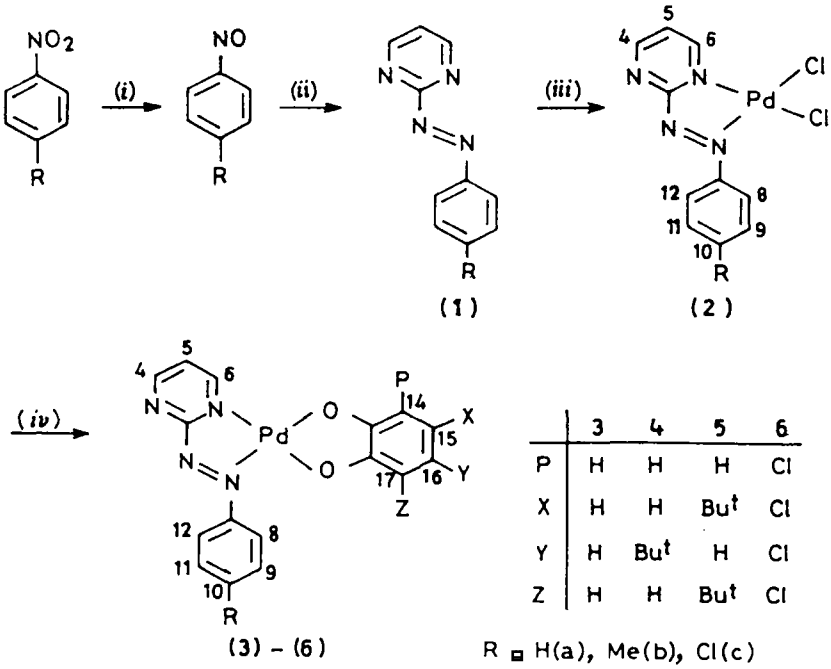

	3	4	5	6
P	H	H	H	Cl
X	H	H	Bu^t	Cl
Y	H	Bu^t	H	Cl
Z	H	H	Bu^t	Cl

(i) Zn/NH_4Cl, $Na_2Cr_2O_7/H_2SO_4$; *(ii)* 2-Aminopyridine in Na/benzene (dry); *(iii)* *cis*-$Pd(CH_3CN)_2Cl_2$ in acetonitrile (CH_3CN); *(iv)* catechols in $CHCl_3$-CH_3OH (1:1, v/v), Et_3N.

Fig. 1. Synthetic Scheme for the Preparation of Compounds (1)-(6).

frequency in catecholate complexes may be attributed to the extensive backbonding d(Pd) → π^*(aapm)[18] or charge transfer transition from a catecholate σ/π-donor center to π^*(aapm), $3b_1$ (cat)→ π^*(aapm)[19]. This is in support of our previous observation[5,6]. The significant vibrations are collected in Table I. The binding of catechols is depicted by the appearance of C-O stretching vibrations at 1480-1450 and 1280-1300 cm^{-1}. The Pd-O stretching vibration appears at 520 cm^{-1}. The disappearance of two distinct Pd-Cl stretchings at 365 and 340 cm^{-1} corresponding to the *cis*-$PdCl_2$ configuration[20] in Pd(aapm)Cl_2 (2) is an indirect evidence of catecholato binding.

UV-VIS Spectra. The electronic spectra of [Pd(aapm)(O,O)] (**3**)-(**6**) were recorded in dichloromethane and compared with the spectra of $Pd(aapm)Cl_2$ (**2**). Absorptions below 400 nm are due to the intraligand charge-transfer[1,2] ($n\rightarrow\pi^*$ and $\pi\rightarrow\pi^*$) and are not considered further. The most significant feature of the spectra is the appearance of a new and broad band in the near-infrared (NIR) region. The position and symmetry are highly dependent on the nature of the substituent in the catechol and azopyrimidine moieties. The data are collected in Table I. Two absorptions are observed above 800 nm for [Pd(aapm)(cat)] (**3**), [Pd(aapm)(tbcat)] (**4**) and [Pd(aapm)(tccat)] (**6**), a main band and a weak shoulder. The shoulder appears at the longer wave length side of the main band. The absorption behaviour of [Pd(aapm)(dtbcat)] (**5**) is somewhat different from that of compounds (**3**), (**4**) and (**6**). Two well-defined absoptions are observed above 1150 nm with a weak shoulder at the higher energy side. The observed trend of the band maxima for a particular azopyrimidine moiety is tccat (**6**) > cat (**3**) > tbcat (**4**) > dtbcat (**5**) (Fig. 2). The observation is corroborated by our earlier results[5,6]. The MO diagram described for [M(α-diimine)(O,O)] (M = Ni(II), Pd(II), Pt(II)); O,O = catecholates) to explain the strong absorption in the NIR region qualitatively may account for the spectral observation in the present complexes. This model describes that the HOMO is characterised by catecholato orbitals and the LUMO belongs to α-diimine groups. The charge transfer transition is characterised as HOMO → LUMO. The energy of this band decreases when electron donor groups are present on the catechol moiety. These results are to be expected when the HOMO of the dtbcat complex (**5**) has the highest energy in the series because of the electron releasing effect of Bu-t groups. In [Pd(aapm)(tccat)] (**6**) the HOMO energy is lower than that of [Pd(aapm)(cat)] (**3**) because of the electron withdrawing effect of the chloro groups. The substitution in the azopyrimidine fragment also shifts the band maxima, in the order *p*-tapm (**b**) > papm (**a**) > *p*-Clpapm (**c**). This is certainly due to the lowering of the energy of the LUMO in [Pd(*p*-Clpapm)(O,O)] (**c**) compared to [Pd(papm)(O,O)] (**a**) because of the

Table I. Microanalyses, IR[b] and Electronic[c] Spectra of the Complexes

Compound (Empirical Formula)	F. W.	Mp[a] (dec)	Yield %	% C Found (Calcd.)	% H Found (Calcd.)	% N Found (Calcd.)	ν(N=N)	ν(C-O)	ν(Pd-O)	λ_{max} (nm) (ε/dm^3 mol^{-1} cm^{-1})
Pd(papm)Cl_2, ($C_{10}H_8N_4Cl_2Pd$) (**2a**)	361.5	>400	85	33.10 (33.20)	2.20 (2.21)	15.42 (15.49)	1380 s			388 (5249), 300 (11202)
Pd(*p*-tapm)Cl_2, ($C_{11}H_{10}N_4Cl_2Pd$) (**2b**)	375.5	>408	80	35.10 (35.16)	2.59 (2.66)	14.85 (14.92)	1385 s			405 (4740), 315 (15018)
Pd(*p*-Clpapm)Cl_2 ($C_{10}H_7N_4Cl_3Pd$) (**2c**)	396.0	>413	90	30.23 (30.31)	1.65 (1.76)	14.20 (14.15)	1380 s			404 (7960), 304 (19801)
Pd(papm)(cat) ($C_{16}H_{12}N_4O_2Pd$) (**3a**)	398.4	>415	74	48.25 (48.19)	3.10 (3.01)	14.00 (14.06)	1340 s	1250 s	500 m	1240 (840)[d], 1050 (1580)[e], 631 (896)
Pd(papm)(tbcat) ($C_{20}H_{20}N_4O_2Pd$) (**4a**)	454.4	>410	63	52.90 (52.82)	4.32 (4.40)	12.25 (12.32)	1330 s	1250 s	505 m	1310 (1190)[d], 1110 (3060)[e], 729 (462)
Pd(papm)(dtbcat) ($C_{24}H_{28}N_4O_2Pd$) (**5a**)	510.4	>418	55	56.30 (56.42)	5.40 (5.48)	10.86 (10.97)	1325 s	1260 s	515 m	1400 (5450), 1175 (4800)[e], 1019 (1596), 469 (4550)
Pd(papm)(tccat) ($C_{16}H_8N_4O_2Cl_4Pd$) (**6a**)	536.4	>426	79	35.64 (35.79)	1.43 (1.49)	10.30 (10.43)	1340 s	1255 s	515 m	1010 (750)[d], 886 (1773)[e], 830 (1262)
Pd(*p*-tapm)(cat) ($C_{17}H_{14}N_4O_2Pd$) (**3b**)	412.4	>423	70	49.35 (49.46)	3.30 (3.39)	13.60 (13.57)	1330 s	1260 s	510 m	1205 (1060)[d],980 (2840)[e], 619 (1860)

Pd(*p*-tapm)(tbcat) ($C_{21}H_{22}N_4O_2Pd$) (**4b**)	468.4	>435	59	53.72 (53.80)	4.75 (4.69)	11.86 (11.95)	1325 s	1265 s	515 m	1240 (1355)[d],1044 (1580)[e], 473 (4823)
Pd(*p*-tapm)(dtbcat) ($C_{25}H_{30}N_4O_2Pd$) (**5b**)	524.4	>443	54	57.30 (57.20)	5.63 (5.72)	10.60 (10.67)	1325 s	1260 s	520 m	1350 (7800), 1160 (5960)[e], 825 (1804), 515 (4420)
Pd(*p*-tapm)(tccat) ($C_{17}H_{10}N_4O_2Cl_4Pd$) (**6b**)	550.4	>434	74	37.00 (37.06)	1.78 (1.82)	10.20 (10.17)	1330 s	1265 s	520 m	975 (2000)[e], 949 (1855), 430 (5700)
Pd(*p*-Clpapm)(cat) ($C_{16}H_{11}N_4O_2ClPd$) (**3c**)	432.9	>421	84	44.40 (44.35)	2.48 (2.54)	12.87 (12.93)	1340 s	1255 s	500 m	1300 (1180),1070 (1890)[e], 652 (1200)
Pd(*p*-Clpapm)(tbcat) ($C_{20}H_{19}N_4O_2ClPd$) (**4c**)	488.9	>445	70	49.16 (49.08)	3.80 (3.88)	11.34 (11.45)	1330 s	1260 s	505 m	1340 (1262), 1145 (3345)[e], 675 (1190), 460 (4795)
Pd(*p*-Clpapm)(dtbcat) ($C_{24}H_{27}N_4O_2ClPd$) (**5c**)	544.9	>437	65	52.96 (52.85)	4.90 (4.95)	10.19 (10.27)	1325 s	1250 s	510 m	1450 (6750), 1228 (5255)[e], 1022 (2428), 549 (3320)[d], 464 (4680)
Pd(*p*-Clpapm)(tccat) ($C_{16}H_7N_4O_2Cl_5Pd$) (**6c**)	570.9	>454	88	33.70 (33.63)	1.20 (1.22)	9.69 (9.80)	1340 s	1260 s	500 m	1035 (855), 870 (1355)[e], 419 (2680)

[a] Decomposition starts at this temperature, [b] In KBr; [c] In CH_2Cl_2; [d] Shoulder; [e] λ used for the calculation of the LLCT transition energy in Table III.

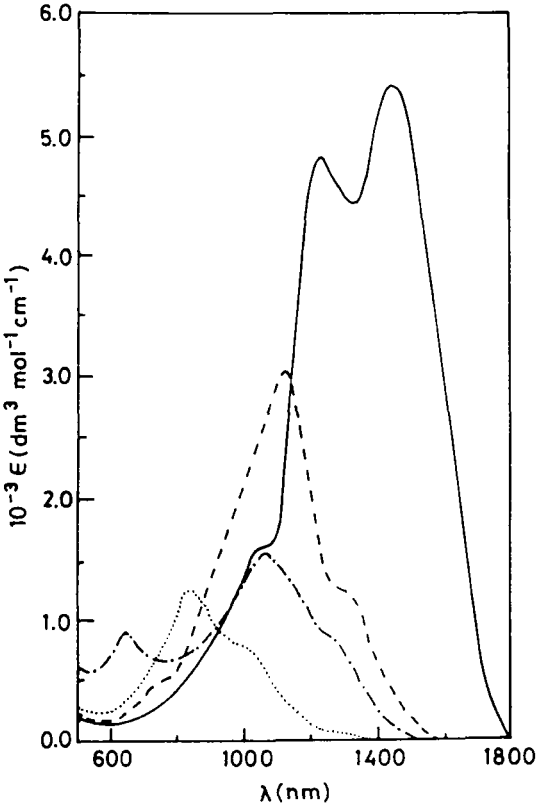

Fig. 2. Electronic Spectra of [Pd(papm)(cat)] (-·-·-), [Pd(papm)(tbcat)] (----), [Pd(papm)(dtbcat)] (—) and [Pd(papm)(tccat)] (·····) in CH_2Cl_2 at 298 K.

electron withdrawing character of chloro groups. The reverse is seen for [Pd(*p*-tapm)(O,O)] (**b**). Thus, the bands are assigned to ligand-to-ligand charge transfer (LLCT)[15,16,21] transitions involving the HOMO of catechols and the LUMO of azopyrimidines. On comparison with the MO diagram of [Pd(α-diimine)(O,O)] the transition may be described as $3b_1(cat) \rightarrow \pi^*(aapm)$[19,22,23]. The solvatochromic behaviour of this transition is under scrutiny.

^{1}H NMR Spectra

The ^{1}H NMR spectra of [Pd(aapm)(O,O)] (**3**)-(**6**) were measured in $CDCl_3$ with Me_4Si as internal reference and were compared with $Pd(aapm)Cl_2$ (**2**). The atom numbering pattern of the complexes is given in Fig. 1. The signals were assigned on the basis of chemical shifts, spin-spin interaction and their effect on substitution. The data are listed in Table II. Representative NMR spectra are shown in Fig. 3. The schematic diagram is shown in Fig. 4. In the present series of complexes (**3**)-(**6**) the arylazopyrimidine protons experience an upfield shift compared with the parent chloro compounds (**2**). This may be due to the stronger binding of the catecholato group to Pd(II) than that of the chloride ions or more back-bonding offered by the azopyrimidine function[15,16,20]. The aromatic protons are divided into two parts. Downfield signals are due to azopyrimidine protons (4-H-6-H). Upfield signals originate from catecholato protons (14-H-17-H) and between these two extremes the aryl proton (8-H-12-H) signals are observed. This is expected in view of the π-acidity of a pyrimidine ring and electron donor effect of the phenolic oxygen in a catechol ring[24].

For the pyrimidine protons, the 6-H signal appears at the most downfield range (8.8-8.9 ppm) as a doublet and the 4-H peak appears at a slightly upfield position (8.6-8.7 ppm). The 5-H signal is observed as a triplet at 8.2-8.3 ppm. The aryl ring protons (8-H-12-H) are perturbed in an expected order by the substituent 10-R. The 10-Me substitution (**b**) shifts the ring protons upfield due to the electron donating effect *via* the inductive effect and the reverse is shown in 10-Cl substituted products (**c**)[25]. The most perturbed signals are the 9-H and 11-H signals. The signal at the most upfield region is assigned to a catecholato proton. [Pd(aapm)(cat)] (**3**) gives a characteristic AA'BB' pattern for the catecholato 14-H-17-H. [Pd(aapm)(tbcat)] (**4**) exhibits a singlet (17-H) and two doublets (14-H and 15-H). [Pd(aapm)(dtbcat)] (**5**) indicates two singlets corresponding to 14-H and 16-H protons.

Table II. ^{1}H NMR Data[a] of the Complexes

Compd.	δ, ppm													
	4-H[b]	5-H[c]	6-H[b]	8-H[b]	9-H	10-H	11-H	12-H[b]	14-H	15-H	16-H	17-H	10-Me	Bu-t
(2a)	8.84	8.49	9.10	7.70	7.53[c]	7.60[c]	7.53[c]	7.81						
(2b)	8.80	8.36	9.02	7.51	7.32[b]		7.32[b]	7.59					2.55	
(2c)	8.88	8.54	9.15	7.76	7.70[b]		7.70[b]	7.85						
(3a)	8.60	8.21	8.80	7.66	7.42[c]	7.60[c]	7.42[c]	7.66	6.82[b]	7.08[c]	7.08[c]	6.82[b]		
(4a)	8.62	8.24	8.78	7.62	7.40[c]	7.55[c]	7.40[c]	7.62	6.73[d]		6.58[b]	6.80[b]		1.34[e]
(5a)	8.60	8.20	8.72	7.60	7.52[c]	7.60[c]	7.52[c]	7.60		6.55[d]		6.80[d]		1.40[f],1.32[g]
(6a)	8.71	8.28	8.91	7.72	7.55[c]	7.68[c]	7.55[c]	7.72						
(3b)	8.63	8.22	8.83	7.40	7.27[b]		7.27[b]	7.40	6.79[b]	7.02[c]	7.02[c]	6.79[b]	2.39	
(4b)	8.60	8.20	8.80	7.45	7.29[b]		7.29[b]	7.45	6.69[d]		6.54[b]	6.74[b]	2.38	1.44[e]
(5b)	8.52	8.18	8.74	7.51	7.48[b]		7.48[b]	7.51		6.60[d]		6.78[d]	2.35	1.42[f],1.31[g]
(6b)	8.70	8.29	8.90	7.54	7.35[b]		7.35[b]	7.54					2.44	
(3c)	8.69	8.29	8.90	7.74	7.66[b]		7.66[b]	7.74	6.84[b]	7.10[d]	7.10[d]	6.84[b]		
(4c)	8.65	8.26	8.85	7.70	7.63[b]		7.63[b]	7.70	6.75[d]		6.60[b]	6.80[b]		1.35[e]
(5c)	8.64	8.24	8.86	7.72	7.60[b]		7.60[b]	7.72		6.70[d]		6.84[d]		1.42[f],1.30[h]
(6c)	8.70	8.32	8.92	7.78	7.66[b]		7.66[b]	7.78						

[a] In $CDCl_3$; [b] Doublet (coupling constants are in the range 7.0-9.0 Hz), [c] Triplet (coupling constants are in the range 7.0-8.0 Hz), [d] Singlet, [e] δ (15-Bu-t), [f] δ (16-Bu-t), [g] δ (14-Bu-t), [h] δ (OH).

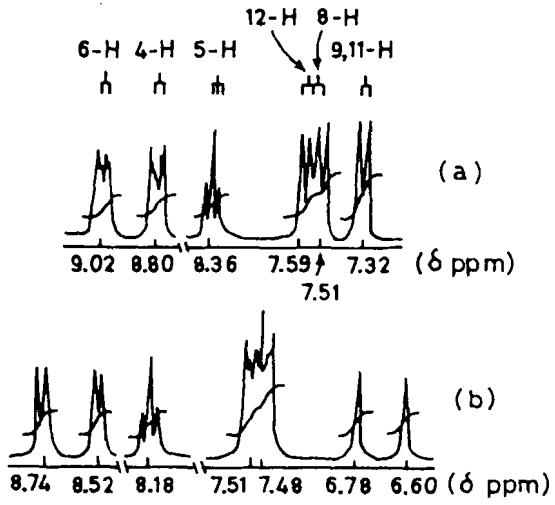

Fig. 3. ^{1}H NMR Spectra of (a) [Pd(*p*-tapm)Cl_2] (**2b**) and (b) [Pd(*p*-tapm)(dtbcat)] (**5b**) in $CDCl_3$ at 298 K.

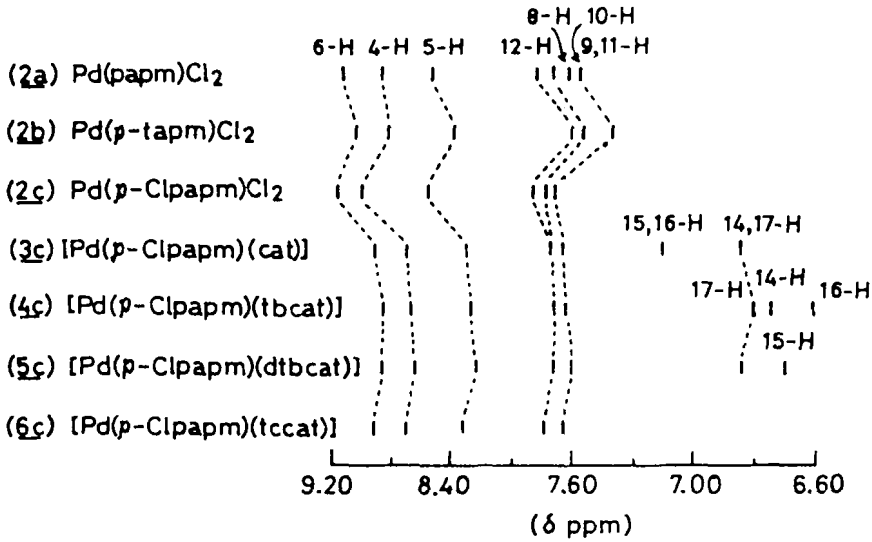

Fig. 4. Schematic ^{1}H NMR Spectra of the Complexes.

Electrochemical Properties

All measurements were carried out using a glassy carbon working electrode and a Pt-wire as auxiliary electrode. Potentials are expressed with reference to a saturated calomel electrode (SCE). Tetrabutylammonium perchlorate, $[Bu_4N][ClO_4]$, was used as the supporting electrolyte. Cyclic voltammetric data are summarized in Table III.

[Pd(aapm)(O,O)] (**3**)-(**6**) exhibit three or four reversible or quasi-reversible redox processes within the potential range +1.5 to -1.5 V *versus* SCE. Two responses at the negative side to SCE are due to azo reductions. On comparison with the related system we may conclude that the LUMO of aapm may accommodate upto two electrons[26]. The reduction may be considered as electron acceptance at the azo function [eqs (1) and (2)]. Similar reductive responses in $[Pd(aapm)Cl_2]$ (**2**) were observed at the less negative potential.

$$[-N = N-] \overset{+e}{\rightleftharpoons} [-N\text{—}N-]^{\cdot -} \qquad (1)$$

$$[-N\text{—}N-]^{\cdot -} \overset{+e}{\rightleftharpoons} [-N\text{—}N-]^{2-} \qquad (2)$$

The potentials are linearly correlated with Hammett σ of the substituents. The reduced species does not appear to be stable and on scan reversal the counter peak appears at the large difference in the potential .

In the positive scan to SCE, the complexes [Pd(aapm)(O,O)] (**3**)-(**6**) show two successive one-electron oxidation processes with varying degree of reversibility (*Fig. 5*) depending upon the substituents on the catecholato ring. In [Pd(aapm)(tbcat)] (**4**) and [Pd(aapm)(dtbcat)] (**5**) the first oxidation process [eq (3)] is perfectly reversible and the second oxidation [eq (4)] is found to be reasonably reversible.

(3)

Table III. Cyclic Voltammetric Data[a] for Complexes (2)-(6)

Compd.	$E^3_{1/2}$ (ΔE_p, mV) cat/sq	$E^4_{1/2}$ (ΔE_p, mV) sq/q	$E^1_{1/2}$ (ΔE_p, mV) azo^-/azo	$E^2_{1/2}$ (ΔE_p, mV) azo^{2-}/azo^-	$\Delta E^b_{1/2}$, V	$\bar{\nu}_{LLCT}$[c], eV
(2a)			-0.018 (140)	-1.090[e]		
(2b)			-0.122 (160)	-1.157[e]		
(2c)			-0.105 (100)	-0.920[e]		
(3a)	0.59 (90)	1.18[d]	-0.18 (85)	-0.78 (120)	0.77	1.182
(4a)	0.50 (70)	1.09 (100)	-0.24 (90)	-0.89 (130)	0.74	1.118
(5a)	0.43 (75)	0.98 (110)	-0.32 (70)	-1.04 (100)	0.75	1.056
(6a)	0.73 (65)	1.23[d]	-0.03 (90)	-0.78 (120)	0.76	1.400
(3b)	0.54 (80)	1.09[d]	-0.27 (90)	-1.07 (110)	0.81	1.266
(4b)	0.45 (70)	0.93 (110)	-0.33 (90)	1.19 (100)	0.78	1.224
(5b)	0.38 (75)	0.90 (120)	-0.41 (85)	-1.16 (110)	0.79	1.080
(6b)	0.70 (70)	1.19[d]	-0.11 (90)	-0.86 (120)	0.81	1.273
(3c)	0.64 (80)	1.24[d]	-0.11 (80)	-0.75 (130)	0.75	1.159
(4c)	0.57 (65)	1.14 (80)	-0.15 (90)	-0.83 (110)	0.72	1.093
(5c)	0.48 (100)	1.01 (100)	-0.24 (80)	1.10 (140)	0.72	1.035
(6c)	0.81 (160)	1.41[d]	0.04 (70)	-0.70 (100)	0.85	1.426

[a] In CH_2Cl_2:CH_3CN (1:3, v/v), supporting electrolyte $[Bu_4N][ClO_4]$, Pt-milli disk working electrode, Pt-wire auxiliary electrode, solute concentration *ca* 10^{-3}, scan rate 50 mVs^{-1}, potentials are in V *versus* SCE; $E_{1/2} = (E_{pa} + E_{pc})/2$, $\Delta E_p = E_{pa} - E_{pc}$; [b] $\Delta E_{1/2} = (E^3_{1/2} - E^1_{1/2})$; [c] $\bar{\nu}_{LLCT} = 1241/\lambda$ (nm), eV where λ is collected from Table I; [d] E_{pa} values; [e] E_{pc} values.

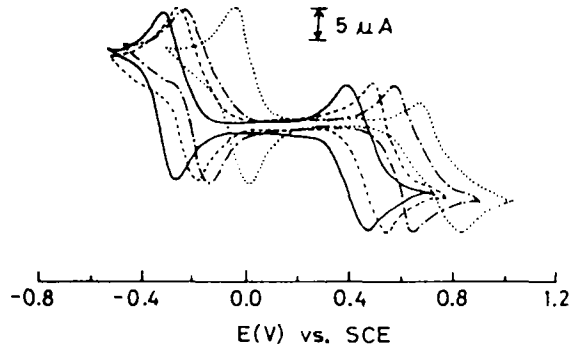

Fig. 5. Cyclic Voltammogram of [Pd(papm)(cat)] (-·-·-), [Pd(papm)(tbcat)] (----), [Pd(papm)(dtbcat)] (——) and [Pd(papm)(tccat)] (·····) in CH_3CN Using GC-Disk Milli Electrode at 298 K.

(4)

An irreversible second oxidation process is observed with [Pd(aapm)(cat)] (**3**) and [Pd(aapm)(tccat)] (**6**). This is because of electron withdrawing substituents in the catecholato ring. The oxidations are catecholato to semiquinone [Rcq/Rsq, eq (3)] and semiquinone to quinone [Rsq/Rq, eq (4)]. The presence of Bu-t group(s) in the ring efficiently stabilizes the cation radical, possibly through a hyperconjugative effect[27] in the complexes (**4**) and (**5**). On the other hand, in the complexes (**3**) and (**6**) catechols are oxidized irreversibly because of the lack of sufficient electron influx to the semiquinone ring which may be needed for the cation radical stabilization[26].

Spectro-Electrochemical Correlation

The ligand-to-ligand charge transfer (LLCT) transition appears at the near-IR

region of 850-1300 nm. The electrochemical studies exhibit reversible redox responses corresponding to Rsq/Rcq and azo/azo˙ in the potential range 0.5 to 0.8 V and 0.0 to -0.4 V *versus* SCE, respectively. The oxidation response is due to electron extraction from HOMO dominated by a catechol group $3b_1$(cat) and the reduction is the electron accommodation at LUMO characterized by the azo function. The LLCT transition is suggested as $3b_1(cat) \rightarrow \pi^*$ (aapm)[19,22,23]. Therefore, there may exist a linear correlation between the energy of the main LLCT transition and the potential difference [eq (5)] of the first oxidation [(eq (3)] and first reduction potential [eq (1)]. The plot follows the linear eq (5) (Fig. 6).

$$\bar{\nu}_{LLCT} = 2.33\ \Delta E_{1/2} - 0.60 \qquad (5)$$

($\Delta E_{1/2} = E^3_{1/2} - E^1_{1/2}$, where $E^3_{1/2}$ and $E^1_{1/2}$ refer to the redox potential of eq (3) and eq (1), respectively)

EXPERIMENTAL

Materials

Palladium chloride was obtained from Arora Mathey Company, Calcutta. 2-(Arylazo)pyrimidines were synthesised by condensing 2-aminopyrimidine with appropriate nitrosoaromatics according to the published procedure[1,2]. Pyrocatechol (H_2cat), 3,5-di-*tert*-butylcatechol (H_2dtbcat) and tetrachlorocatechol (H_2tccat) were obtained from Aldrich Chemicals. 4-*tert*-Butylcatechol (H_2tbcat) was received from Fluka Chemie. Catechols were purified by recrystallization from benzene. Acetonitrile and dichloromethane were further purified by distillation over P_4O_{10}. Commercial grade silica gel (60-120 mesh), from Sisco Research Lab, was used for column chromatography. Nitrogen was purified by successively bubbling through an alkaline pyrogallol solution and concentrated sulfuric acid. Tetrabutylammonium perchlorate was prepared and recrystallized

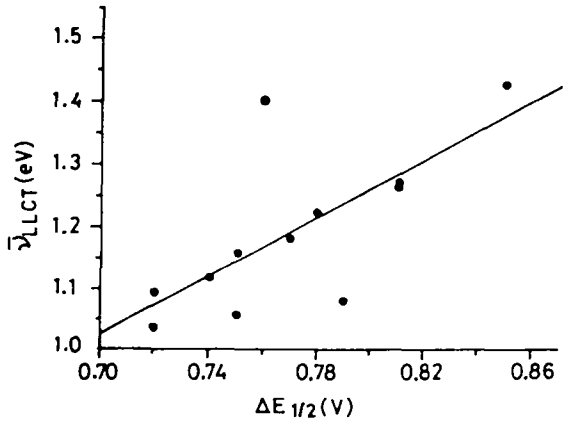

Fig. 6. Spectro-Electrochemical Correlation Plot of $\Delta E_{1/2}$ (V) *vs.* $\bar{\nu}_{LLCT}$ (eV).

by a previously reported method[21]. Triethylamine, all other chemicals and solvents used for the preparative works were reagent grade and were used as received.

Physical Measurements

The IR spectra (200-4000 cm^{-1}) were recorded as KBr discs using a JASCO FTIR 420 spectrophotometer. UV-Vis spectra were measured on Shimadzu UV-160A and Hitachi U-3501 spectrophotometers in dichloromethane solutions. ^1H NMR spectra were recorded on a Brucker 300 MHz FT-NMR in chloroform-d solutions. Electrochemical studies were performed on a computer-controlled EG & G PAR model 270 VERSTAT electrochemical instrument. Potentials were measured with reference to a standard calomel electrode (SCE) using a glassy carbon microelectrode as working and Pt wire as auxiliary electrode and were uncorrected for junction potentials. Bu_4NClO_4 was used as a supporting electrolyte. Microanalytical data were obtained by a Perkin-Elmer 2400 CHN analyzer.

Synthesis of Complexes

The complexes were prepared using similar methods[5]. Details of representative complexes are shown below.

Dichloro-[2-(phenylazo)pyrimidine]palladium(II) Pd(papm)Cl_2 (**2a**)

To a CH_3CN (10 mL) solution of $PdCl_2$ (0.18 g, 1.01 mmol), 2-(phenylazo)pyrimidine (**1a**) (0.2 g, 1.09 mmol) was added gradually and the mixture was stirred for 1 h at 298 K. The orange-red precipitate formed was recovered by filtration and washed with CH_3OH. The dried product was dissolved in CH_2Cl_2 and purified by chromatography on a silica gel (60-120 mesh) column. The desired orange-red band was eluted by CH_3CN-C_6H_6 (30 % v/v). The yield was 0.3 g (85 %).

Catecholato-[2-(phenylazo)pyrimidine]palladium(II) [Pd(papm)(cat)] (**3a**)

Pd(papm)Cl_2 (**2a**) (0.3 g, 0.83 mmol) was dissolved in $CHCl_3$-CH_3OH (50% v/v, 20 mL) and the solution was degassed by bubbling N_2 through it. To this solution was added slowly catechol (0.1 g, 0.91 mmol) in CH_3OH (10 mL) followed by Et_3N (2 mmol) under N_2. The solution was stirred for 1 h at 298 K and N_2 gas was passed into it for another 1 h to reduce its original volume to one-third. At this stage a brown-violet precipitate slowly separated. It was removed by filtration and washed with H_2O and CH_3OH and dried *in vacuo*. The residue was dissolved in CH_2Cl_2 and chromatographed on a silica gel column. The desired compound was eluted by CH_3CN-C_6H_6 (20 %, v/v). Evaporation of the solvent gave a pure crystalline brown-violet coloured product. The yield was 0.3 (74 %).

ACKNOWLEDGEMENTS

We thank the University Grants Commission, New Delhi, for financial assistance. Our sincere thanks are due to Prof. G. N. Mukherjee, Department of

Chemistry, Calcutta University, Calcutta, India, for recording some UV-VIS-NIR spectra and Dr. B. B. De, University of Massachusetts, Lowell, USA for some ^1H NMR spectra.

REFERENCES

1. P. K. Santra, D. Das, T. K. Misra, R. Roy, C. Sinha and S.-M. Peng, Polyhedron, 18, 1909 (1999).

2. P. K. Santra, T. K. Misra, D. Das, C. Sinha, A. M. Z. Slawin and J. D. Woollins, Polyhedron, 18, 2869 (1999).

3. T. K. Misra, D. Das, C. Sinha, P. Ghosh and C. K. Pal, Inorg. Chem., 37, 1672 (1998).

4. T. K. Misra, D. Das and C. Sinha, Polyhedron, 16, 4163 (1997).

5. D. Das and C. Sinha, Transition. Met. Chem., 23, 517 (1998).

6. R. Roy, P. Chattopadhyay, C. Sinha and S. Chattopadhyay, Polyhedron, 15, 3361 (1996).

7. D. Das, A. K. Das and C. Sinha, Talanta, 48, 1031(1999), Anal. Lett., 32, 567 (1999).

8. E. C. Constable, Coord. Chem. Rev., 93, 205 (1989).

9. J. K. Nag, T. K. Misra and C. Sinha, Indian J. Chem., 36A, 951 (1997).

10. S. Patai, Ed., "The Chemistry of Quinoid Compounds, Parts 1 and 2", Wiley, New York (1974).

11. R. H. Thompson, "Naturally Occurring Quinones, III, Recent Advances", Chapman and Hall, London (1987).

12. R. A. Morton, Ed., "Biochemistry of Quinones", Academic Press, New York (1965).

13. G. A. Fox and C. G. Pierpont, J. Chem. Soc., Chem. Commun., 806 (1988).

14. S. Bhattacharya, S. R. Boone, G. A. Fox and C. G. Pierpont, J. Am. Chem. Soc., 112, 1088 (1990).

15. S. S. Kamath, V. Uma and T. S. Srivastava, Inorg. Chim. Acta, 166, 91 (1989).

16. V. Anbalagan and T. S. Srivastava, Polyhedron, 13, 291 (1994).

17. S. D. Cummings and R. Eisenberg, Inorg. Chem., 34, 2007 (1995).

18. D. Datta and A. Chakravorty, Inorg. Chem., 22, 1085 (1983).

19. K. C. Kalia and A. Chakravorty, J. Org. Chem., 35, 2231 (1970).

20. C. K. Pal, S. Chattopadhyay, C. Sinha, D. Bandyopadhyay and A. Chakravorty, Polyhedron, 13, 999 (1994).

21. G. K. Lahiri, S. Goswami, L. R. Falvello and A. Chakravorty, Inorg. Chem., 26, 3365 (1987) and references therein.

22. D. J. Gordon and R. F. Fenske, Inorg. Chem., 21, 2907 (1982) and references therein.

23. M. Haga, E. S. Dodsworth and A. B. P. Lever, Inorg.Chem., 25, 447 (1986) and references therein.

24. C. Sinha, Polyhedron, 12, 2363 (1993).

25. P. Chattopadhyay and C. Sinha, Polyhedron, 13, 2689 (1994).

26. S. Goswami, R. N. Mukherjee and A. Chakravorty, Inorg. Chem., 22, 2825 (1983).

27. S. B. Kumar and M. Chaudhury, J. Chem. Soc., Dalton Trans., 2169 (1991).

Received: 28 September 1999 Referee I: K. Sakata
Accepted: 18 August 2000 Referee II: H. Kuma